

Lawrence Berkeley National Laboratory

Recent Work

Title

JET PHYSICS AT PEP AND PETRA

Permalink

<https://escholarship.org/uc/item/0d71w176>

Author

Hofmann, W.

Publication Date

1987-09-01



Lawrence Berkeley Laboratory

UNIVERSITY OF CALIFORNIA

Physics Division

RECEIVED
LIBRARY
BERKELEY LABORATORY

NOV 16 1987

LIBRARY AND
DOCUMENTS SECTION

Invited talk presented at the SLAC Summer Institute on
Particle Physics, Stanford, CA, August 10-21, 1987

Jet Physics at PEP and PETRA

W. Hofmann

September 1987



LBL-24086
2

DISCLAIMER

This document was prepared as an account of work sponsored by the United States Government. While this document is believed to contain correct information, neither the United States Government nor any agency thereof, nor the Regents of the University of California, nor any of their employees, makes any warranty, express or implied, or assumes any legal responsibility for the accuracy, completeness, or usefulness of any information, apparatus, product, or process disclosed, or represents that its use would not infringe privately owned rights. Reference herein to any specific commercial product, process, or service by its trade name, trademark, manufacturer, or otherwise, does not necessarily constitute or imply its endorsement, recommendation, or favoring by the United States Government or any agency thereof, or the Regents of the University of California. The views and opinions of authors expressed herein do not necessarily state or reflect those of the United States Government or any agency thereof or the Regents of the University of California.

Jet Physics at PEP and PETRA

W. Hofmann

Lawrence Berkeley Laboratory
University of California
Berkeley, CA 94720

September 1987

Invited Talk at the
SLAC Summer Institute on Particle Physics
Stanford, CA, August 10-21, 1987

ABSTRACT

Recent data on the fragmentation of quarks at PEP and PETRA energies is discussed in the context of phenomenological models of parton fragmentation. Emphasis is placed on the experimental evidence for parton showers as compared to a fixed order QCD treatment, on new data on inclusive hadron production and on detailed studies of baryon production in jets.

1. INTRODUCTION

The creation of jets of hadrons in e^+e^- annihilation events begins with the production of a pair of primary quarks by the virtual photon produced in the annihilation. Because of the large momentum transfer involved, these quarks are usually highly virtual; they cascade down to the mass shell by successive emission of gluons. Those gluons in turn may be off-shell and branch into two new gluons or another pair of quarks, and so on, until all partons of the cascade are close to their mass shell. This process can be described in perturbative QCD, either in terms of a fixed-order calculation or in terms of a parton "shower"¹. Below a certain virtuality, the relevant coupling constant, α_s , becomes large and perturbative expansions are no longer valid. A non-perturbative mechanism sets in and turns the quarks and gluons of the parton shower into primary hadrons. Finally, these hadrons decay and give rise to the observed stable particles. The main goals behind the physics of jets are thus to test techniques developed in perturbative QCD, and to derive a deeper knowledge as well as phenomenological models of the nonperturbative regime. As an occasional fringe benefit, we may learn something new about particles and their decays.

In this review of recent results, I will address the following main topics:

- Determination of the strong coupling constant.
- Properties and phenomenological relevance of parton showers as compared to fixed-order calculations in perturbative QCD.
- New results on inclusive hadron production as a test of fragmentation models.
- Ways to probe the dynamics of the hadronization process using baryons.
- New ideas on the phenomenology of the fragmentation process.

2. PHENOMENOLOGY OF PARTON FRAGMENTATION

Let me first review the phenomenology in a little more detail. Concerning the perturbative evolution, I will concentrate on the concept of parton showers. The main features of parton showers are summarized in Fig. 1(a). The evolution of partons towards their mass shell is described as a branching process¹ governed by the Altarelli-Parisi equations², which account for collinear singularities in the leading-log approximation. Over the last years, one has also learned³ to deal with leading infrared singu-

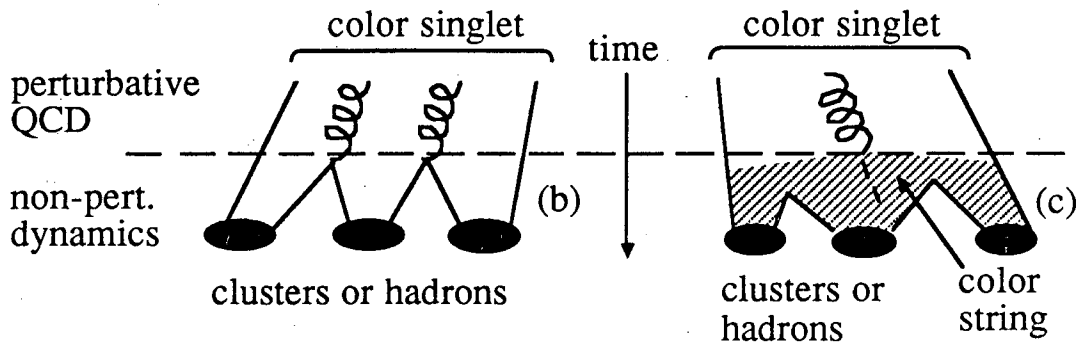
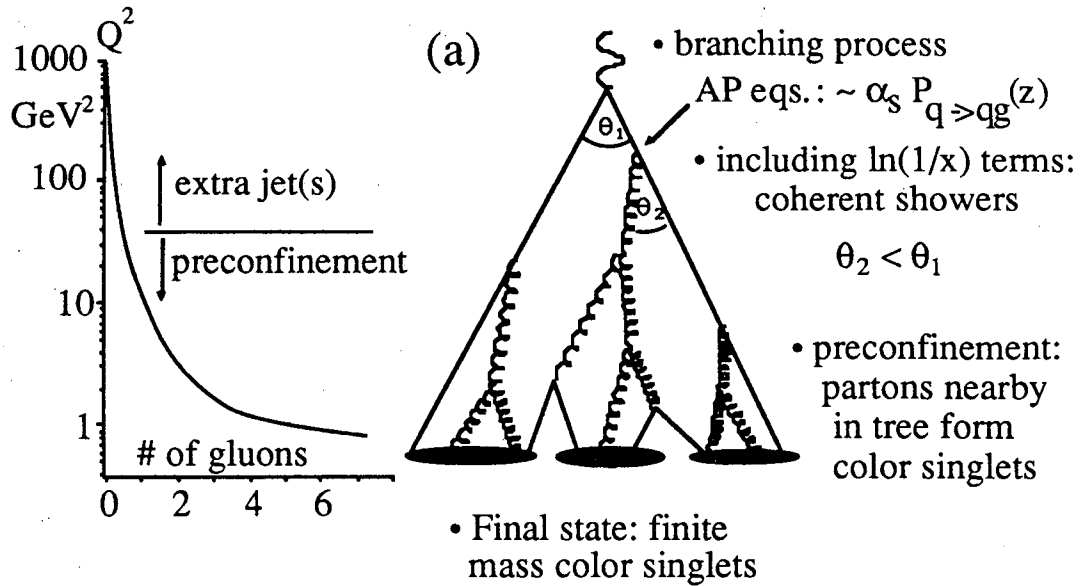


FIGURE 1

(a) Evolution of a parton shower via successive branching, ending with the formation of color singlets. The scale on the left indicates parton virtualities; also shown is the average number of gluons in the shower as a function of the virtuality cutoff Q^2 . (b) Hadronization of color singlet systems in QCD cluster models. (c) Hadronization of color singlet systems in string models

larities; those developments have resulted in the notion of a "coherent" or angular-ordered shower, as compared to "conventional" parton showers. In coherent showers the emission angles decrease monotonically for successive branchings. This additional constraint reduces the phase space for parton emission and effectively accounts for interference effects. This is particularly easy to visualize for the first $q \rightarrow qg$ branching: obviously, by the time the first gluon is emitted, the separation between quark and antiquark must be at least of the order of the gluon wavelength, otherwise quark and antiquark will act as a color singlet and not emit gluons. A short semi-classical calculation shows that (in the infinite-momentum frame) this condition is equivalent to the ordering of angles, $\theta_1 > \theta_2$. Near the end of the shower, angular ordering reduces the phase space for gluon emission and hence the number of soft gluons drastically. Parton showers exhibit another interesting property: preconfinement⁴, a precursor to color confinement within perturbative QCD. Partons nearby in the tree structure can be shown to form color singlets consisting of a quark, an antiquark, and a number of gluons (Fig. 1(a)). The average mass of these singlets approaches a finite limit as the cms energy of the entire cascade increases; this means that at higher energies one will have more of these singlets, but their properties remain the same. Unfortunately, for typical virtuality cutoffs around $Q^2 \approx 1 \text{ GeV}^2$ (at significantly lower values, perturbation theory will break down), the mass of these color singlets is fairly large and the singlets cannot be identified with hadrons. In fact, typical events at PEP or PETRA energies contain one or at most two such color singlet systems. The reason is that the number of singlets is given by $n_{q\bar{q}} + 1$, where $n_{q\bar{q}}$ is the number of new $q\bar{q}$ pairs produced in the shower. Because of the small quark-gluon coupling (compared to the strength of the triple-gluon vertex), quark pair production is a rather infrequent process in a shower, which evolves mainly via $g \rightarrow gg$. The average number of gluons in a parton shower in the PEP/PETRA energy range is shown in Fig. 1(a), as a function of the virtuality cutoff Q^2 ⁵. Above a cutoff around 30 GeV^2 , the gluon multiplicity is small; those gluons will show up as extra jets in the events. At later stages, the number of gluons increases up to 5 to 10 per event; these gluons are no longer visible as extra jets, but they still influence the overall kinematic structure of the events.

In order to model parton fragmentation one has to deal somehow with the color singlet systems resulting from the shower evolution. The fundamental idea is always the same: the starting point is a system made of a quark, an antiquark and the gluon field "in between". Somehow, the gluons will create new quark-antiquark pairs and, following the planar color flow, each quark will have an antiquark neighbor nearby in phase space with which it forms a color singlet state⁴. If the number of new pairs is sufficiently large, the mass of those singlets will be in the GeV range and they can be identified either with known hadrons, or with clusters (excited meson states, some-

what along the lines of Hagedorn's bootstrap model), or with a mixture of both. The two flavors of available models differ mainly in their description of the gluon field: "QCD cluster models"⁶ simply split the gluons remaining after the perturbative evolution into quark-antiquark pairs (or sometimes into diquark-antidiquark pairs) and thus extend the preconfinement mechanism one step further (Fig. 1(b)). Members of this category are the Webber model⁷ and the (meanwhile more or less extinct) Fox-Wolfram⁸, Field-Wolfram⁹, and CALTECH I¹⁰ models. The decay of the clusters is often described as a two-body phase space decay into hadrons or lower-mass clusters, resulting in a refreshingly small number of free parameters (the Webber model has about 5 adjustable parameters, compared to about 15 in the Lund model to be discussed later¹¹).

On the other hand, "string models"^{12,13} describe the gluon field as a classical field (contracted effectively into one dimension due to the non-abelian nature of QCD, hence "string"). Quark and antiquark represent the momentum-carrying ends of the string, and perturbative gluons are viewed as momentum concentrations, or kinks, of the string. In this one-dimensional color field, new quark-antiquark pairs are produced, which screen the field and recombine to form mesons (Fig. 1(c)). The modeling of the string decay closely follows the Schwinger model¹⁴ describing charge screening in a one-dimensional world of massless fermions. The best known representative of this class is the Lund model^{12,15}, which employs a string decaying into mesons and baryons. The CALTECH II¹⁶ model also uses strings which, however, decay mainly into heavy (≈ 2 GeV) hadronic clusters. Cluster decay properties are parametrized¹⁷ based on low-energy data.

3. DETERMINATION OF THE STRONG COUPLING CONSTANT

The evolution of parton showers is governed by the strong coupling constant α_s . I will briefly comment on the status of α_s measurements at PEP and PETRA. Because of the many ambiguities and approximations in the description of parton showers¹⁸, α_s determinations in e^+e^- annihilation usually proceed via the comparison with models based on 2nd-order QCD. This constraint limits the models to string models (SF) such as the Lund model and independent-fragmentation models (IF) such as the Hoyer¹⁹ or Ali²⁰ models. In order to reduce the sensitivity to the modeling, infrared safe measurable, e.g. the asymmetry of energy-energy correlation or planar triple correlations are used. Even for the relatively well-defined 2nd-order calculation, however, the resulting α_s ²¹ proved to be sensitive to details of the QCD calculations (in particular to subleading corrections²² and to the definition of the cutoffs and the parton recombination scheme used to combine unresolvable parton pairs²³), as well as to the choice of the fragmentation model^{24,21}. After some initial confusion, the perturbative side now appears to be better understood; irreducible uncertainties related to the cutoff

scheme (and hence to the interface to the nonperturbative domain) result in an uncertainty in α_s of order $\Delta\alpha_s \approx \pm 0.012$ ²³. Even the infrared safe quantities mentioned above do leave a certain sensitivity to the fragmentation model, of about the same size as the uncertainty due to the perturbative calculation. Statistical errors are negligible compared to these systematics. Latest measurements²⁵ of α_s based on the Lund fragmentation model agree rather well and cluster near $\alpha_s \approx 0.15-0.16$, with an average of 0.156 ± 0.005 . Using independent-fragmentation models, the α_s values are reduced by $0.01-0.02$ ²⁵. Within the systematics discussed above, good agreement is obtained with the α_s value derived from the corrections to the total annihilation cross section, as determined by the CELLO group²⁶ to $\alpha_s = 0.138 \pm 0.023$ based on data from DORIS, PETRA, PEP and TRISTAN.

An essential feature of QCD is the variation of the coupling constant with mass or distance scales. While there is indirect evidence for a running α_s , first direct experimental evidence was presented only very recently by JADE²⁷. The basic idea is very simple: we define (at the parton level) the n -jet rate R_n as the fraction of events with n partons, where the invariant mass M_{ij}^2 of any two partons is greater than a certain fraction of the cms energy, $M_{ij}^2 > ys$. In QCD, R_n is given by

$$R_n = A_n(y) \alpha_s^{n-1} + O(\alpha_s^n) \quad ,$$

where A_n depends only on the dimensionless cutoff y . This equation suggests that if an analogous definition of jets can be used in the experiment, then the (cms-)energy dependence of α_s can be studied directly via the 3-jet rate measured for fixed y (instead of fixed M_{ij}^2 , as usual). Such an analysis has been carried out by the JADE group; their jet finding algorithm initially treats all particles as separate "jets", and then successively forms new jets by collapsing the two jets with the smallest invariant mass into a new jet, until the invariant mass squared M_{ij}^2 of any two jets exceeds a fraction y of the cms energy, $M_{ij}^2 > ys$. The measured R_3 does indeed decrease with increasing \sqrt{s} (Fig. 2); comparison with a model using a constant α_s independent of the cms energy (dashed line) indicates that the observed change in the 3-jet rate cannot be explained by nonperturbative effects. The same model (Lund Jetset 6.3) with a running coupling constant (full line) is in reasonable agreement with the data. While this measurement may not provide the final, model-independent proof of a running α_s (after all, it is hard to demonstrate that *no* fragmentation model can be constructed which has a fixed α_s , and nevertheless agrees with the data shown in Fig. 2 and with all other data on annihilation events), it does provide strong evidence in favor of a running coupling (at present mainly limited by its statistical significance of about 3 S.D.); this is the first time that α_s has been studied over that large an energy range using the same reaction type, analysis technique, and detector.

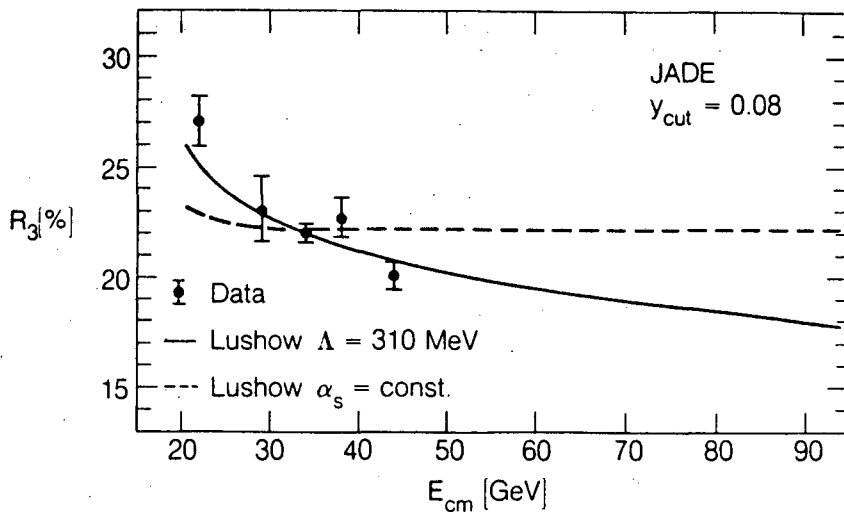


FIGURE 2

Three-jet rate in e^+e^- annihilation as a function of the cms energy \sqrt{s} , for fixed (dimensionless) cutoff $y=0.08$. Dashed and full lines: Lund model (Vs. 6.3) with fixed and running coupling constant, respectively. From JADE²⁷.

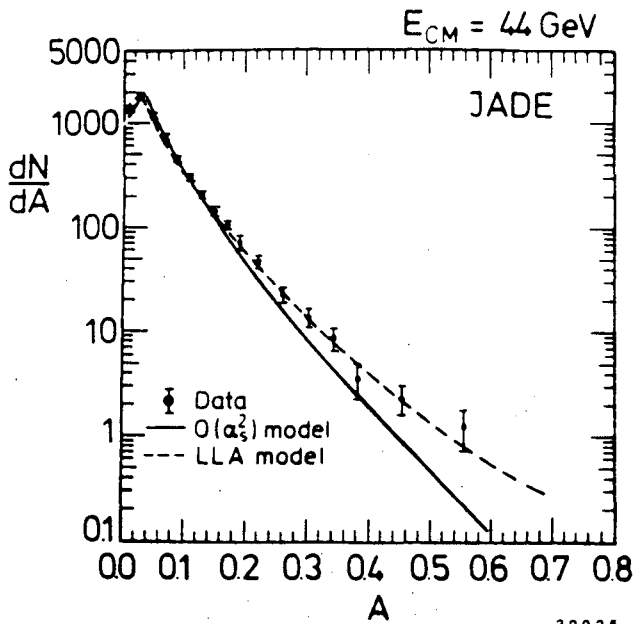


FIGURE 3

Acoplanarity distribution observed in e^+e^- annihilation at 44 GeV. Acoplanarity is defined as $4(\sum |p_{out}| / \sum |p|)^2$, where p_{out} are momentum components out of an event plane chosen to minimize the acoplanarity. Full line: Lund hadronization model using 2nd order QCD matrix elements. Dashed line: Webber hadronization model using parton shower. From JADE²⁸.

4. PHENOMENOLOGICAL RELEVANCE OF PARTON SHOWERS

Let me now address the question of the phenomenological relevance of parton showers at presently available energies, as compared to fixed order calculations in perturbative QCD.

A well known problem in the modeling of e^+e^- annihilation events is an excess of events with large aplanarity, or acoplanarity (the first quantity is a quadratic measure of the momentum flow out of the event plane, the second is linear in momentum), as compared to 2nd order QCD predictions. This is evident from the acoplanarity distribution by JADE²⁸ shown in Fig. 3, which is well described by the parton shower model⁷ (dashed line), but not by the Lund fragmentation model using 2nd order QCD (full line). Since 3-jet events are planar, this observation points towards an underestimate of the rate of 4-jet events in the 2nd order model. This is confirmed by explicit studies of the 2,3,4, and 5-jet frequencies among events. Fig. 4 displays results of a study by JADE²⁸; they were obtained with the jet-finding algorithm discussed above. The n-jet event rates are given in Fig. 4(a) as a function of y . The 2nd order QCD model underestimates the number of 4 and 5 jet events, and at the same time overestimates the number of 3 jet events, indicating that the problem cannot be solved by a readjustment of the strong coupling constant. Changes of the nonperturbative part of the model within the constraints imposed by other data don't improve the agreement either. If the 2nd order QCD parton skeleton of the events is replaced by a parton shower, on the other hand, 4 and 5 jet rates are well reproduced. A disagreement in the 3-jet rate can be traced to the inappropriateness of the LLA in describing the first, large-angle emission of a hard gluon. The JADE analysis is now confirmed by TASSO data²⁹ shown in Fig. 4(b),(c); the techniques and variables used are essentially the same. However, in comparing with shower models, the TASSO group used the most recent version (6.3)¹⁵ of the Lund model, where the shower algorithm is patched to reproduce the $O(\alpha_s)$ result for the $q\bar{q}g$ rate exactly, yielding good agreement with the data for all jet multiplicities and for a wide range of y -values (Fig. 4 (b)) and cms energies (Fig. 4 (c)). From these data sets, it is clear that the fixed-order QCD models do not account for all features of the data; the discrepancies, while relatively small here, will be very significant at SLC or LEP energies.

5. PARTON SHOWERS AND COLOR STRINGS

The distinction between two different phases of the hadronization process - the "perturbative" and the "nonperturbative" phase - is clearly highly artificial and will have to be overcome in any real theory of parton fragmentation. Any hints for a smooth connection between the two phases, as indicated e.g. in the preconfinement phenomenon, represent steps towards a deeper understanding. A recent paper³⁰ can be regarded as a major milestone, since it links coherence effects in parton showers to the

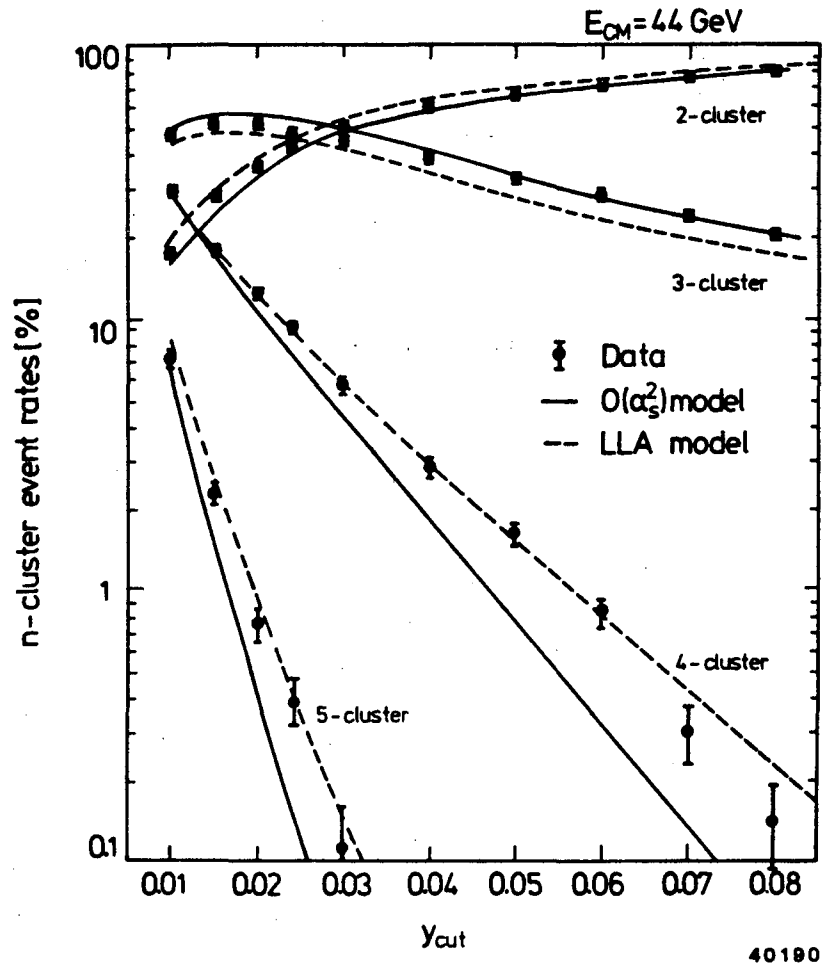


FIGURE 4

(a) Fraction of annihilation events with 2,3,4 and 5 jets (here called "clusters", but not to be confused with the color singlet clusters of QCD), as a function of the cutoff y used in the jet finding algorithm. For a given y , the invariant mass of any pair of jets has to exceed $y\sqrt{s}$. Full line: Lund hadronization model using 2nd order QCD matrix elements. Dashed line: Webber hadronization model using parton shower. From JADE²⁸.

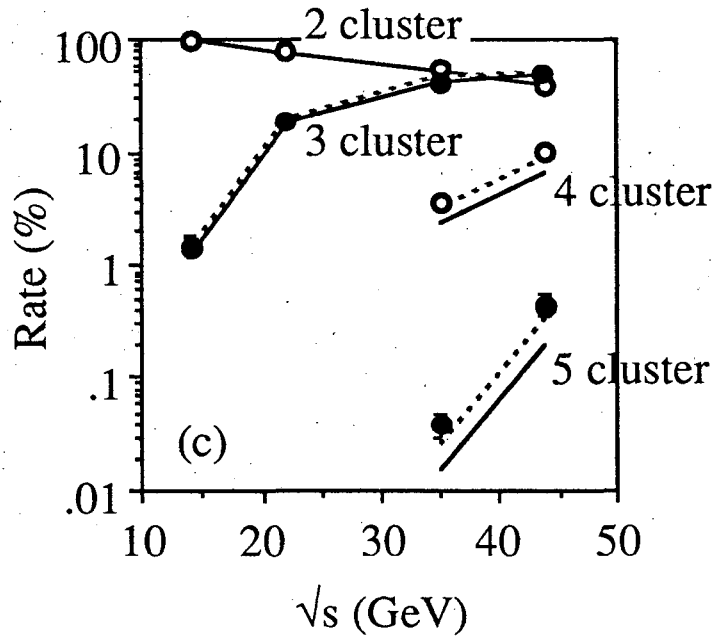
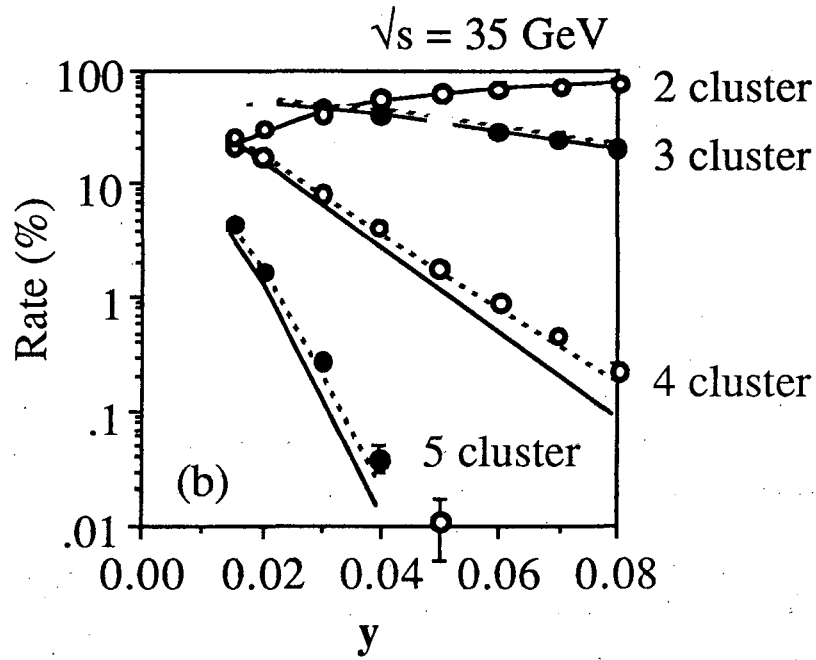


FIGURE 4 (cont.)

(b) Same as (a), but showing TASSO data. (c) Fraction of 2,3,4 and 5 jet events as a function of the cms energy, for a fixed $y=0.04$. Full lines in (b) and (c): Lund hadronization model using 2nd order QCD matrix elements. Dashed line: Lund hadronization model using parton shower with exact $O(\alpha_s)$ cross section. Preliminary TASSO data²⁹.

string model description of quark and gluon fragmentation. The authors investigate the distribution of hadrons in annihilation events with a hard gluon. They assume local duality between hadrons and partons: the angular distribution of hadrons is proportional to the distribution of soft gluons created in the shower evolution. The distribution of such gluons can be derived in analogy to a calculation of soft photon bremsstrahlung in QED; this most naive formalism breaks down for particles near the cores of jets, but should be appropriate for particle emission at large angles. In events with a hard gluon ($q\bar{q}g$), the total angular flow of soft gluons is given by a coherent superposition of soft gluons from quark, antiquark and hard gluon. The explicit calculation reveals an interesting effect: in the angular region between q and \bar{q} , gluon radiation from the different sources interferes destructively, resulting in a reduction of the gluon flow and hence of the hadron flow (Fig. 5). On the other hand, constructive interference takes place in the regions between quark and gluon, and between gluon and antiquark. The resulting polar pattern of the hadron flow in the $q\bar{q}g$ plane is familiar: exactly the same effect is predicted by the string model of parton fragmentation, when used e.g. with 1st order QCD (instead of parton showers): the string is spanned from the quark via the gluon to the antiquark; since each of the two string segments is moving away from the angular region between q and \bar{q} , this region is depleted of hadrons, which are boosted into the $q-g$ and $\bar{q}-g$ regions. In fact, the angular distribution of soft gluon radiation from the $q\bar{q}g$ system equals the angular pattern created by the incoherent superposition of hadron flows from the qg and the $\bar{q}g$ string segments in a string model, up to terms suppressed by $1/N_C$. In other words, the soft gluon interference effects provide a foundation for the string phenomenology!

Furthermore, in Ref. 30 a technique is suggested to test the interference effect in a model independent fashion: one can "switch the destructive interference off" while maintaining the kinematic structure of the events simply by replacing the hard gluon by a hard photon. A comparison of the particle flow in the region between q and \bar{q} should reveal a depletion for $q\bar{q}g$ as compared to $q\bar{q}\gamma$ events. In contrast to earlier tests of the "string effect"³¹ based on a comparison of particle flow in regions 2 and 3 (see Fig. 5), which are kinematically not fully equivalent, the $q\bar{q}g/q\bar{q}\gamma$ comparison can be interpreted without reference to fragmentation models. Data on the $q\bar{q}g/q\bar{q}\gamma$ comparison come from the JADE, TPC and MARK II groups³² (Fig. 6). They plot the ratio of the angular particle flow as a function of the variable x , which maps the angular region between q and \bar{q} onto the interval 0 to 1. The predicted depletion is indeed observed, and is shown to be consistent with string-model predictions (Fig. 7). The new JADE data agree well with the earlier results from the TPC and MARK II detectors.

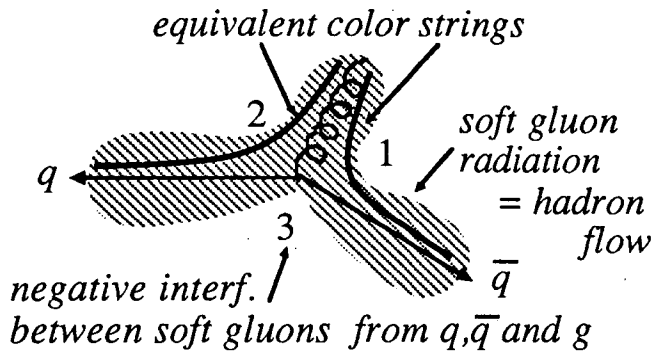


FIGURE 5

Schematic representation of the angular distribution of soft gluons in annihilation events with a hard gluon. Negative interference decreases the amount of gluon radiation into the region between q and \bar{q} (region 3). The same effect is predicted in string models, where a color string is spanned from the quark via the gluon to the antiquark, thus boosting particles away from region 3, into regions 1 and 2.

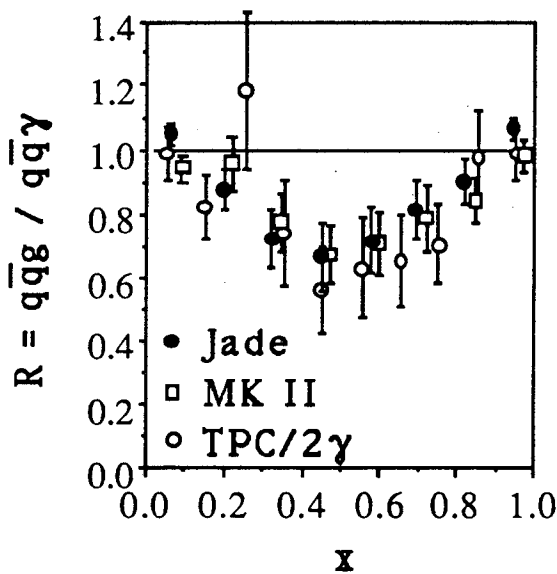


FIGURE 6

Ratio of the particle density in region 3 of three-jet events ($q\bar{q}g$) and radiative annihilation events ($q\bar{q}\gamma$), as a function of the scaled angle $x = \theta_{\text{hadron-jet1}} / \theta_{\text{jet2-jet1}}$. Jets 1 and 2 of $q\bar{q}g$ events are the two highest-energy jets, typically q and \bar{q} . The $q\bar{q}g$ and $q\bar{q}\gamma$ events are selected to have similar kinematics, i.e. similar average momenta and angles of photon and gluon. Shown are data from JADE, MARK II and TPC/2 γ ³².

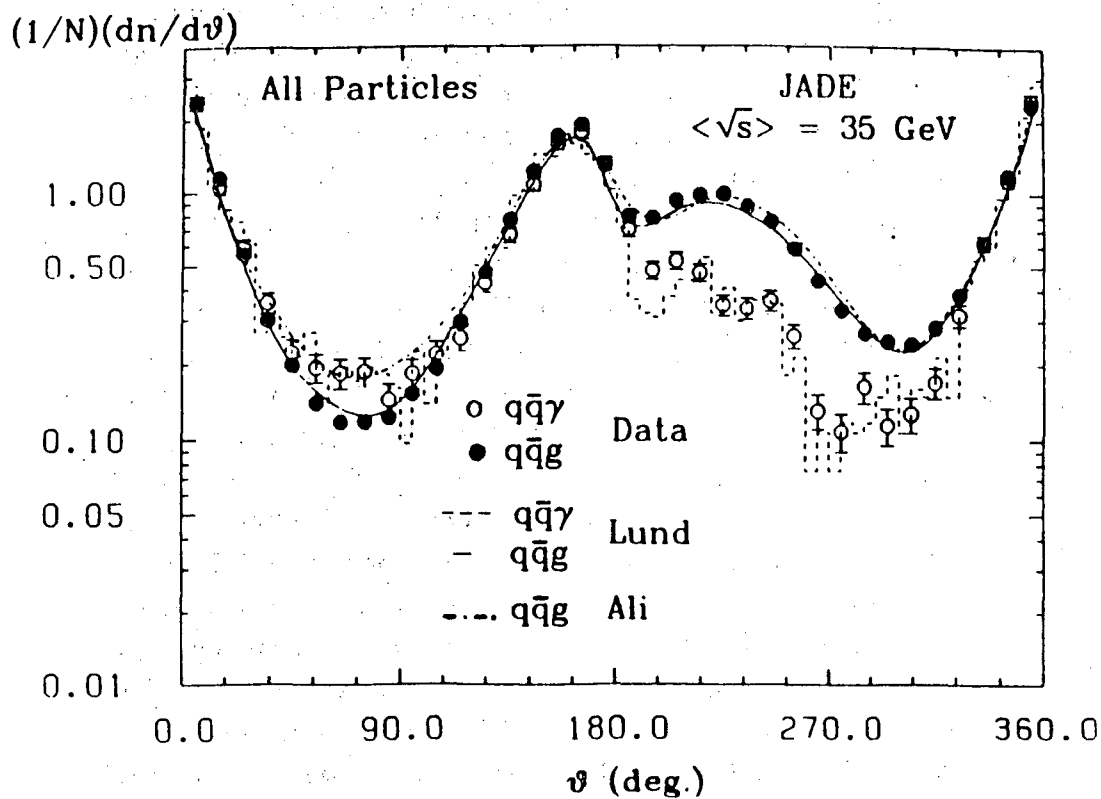


FIGURE 7

Angular flow in the event plane of particles in 3-jet events ($q\bar{q}g$) and in radiative annihilation events ($q\bar{q}\gamma$), as a function of the angle θ between a particle and the highest-momentum jet. The jet with the 2nd-highest momentum is near 160° , the third (gluon) jet or the photon is near 230° . Included are (2nd order QCD) Lund model predictions for $q\bar{q}g$ and $q\bar{q}\gamma$ and predictions of an independent-fragmentation model (Ali) for $q\bar{q}g$. From JADE³².

6. A SHOOT-OUT OF FRAGMENTATION MODELS

In an attempt to identify the features required for a successful phenomenological description of parton fragmentation, the MARK II group has compared several fragmentation models with an exhaustive set of data on inclusive particle distributions and event shape variables³³. Relevant parameters of the models were tuned such as to optimize the agreement with the MARK II data. (Not surprisingly, the resulting parameter values were in most cases close to their default settings supplied by the authors of the models.) Fig. 8 shows the distributions in aplanarity and thrust, compared to i) the Lund string model (version 6.3) with coherent parton showers, ii) the string model with 2nd order QCD, iii) an updated version (4.1) of the Webber model⁷, based on parton showers creating clusters and iv) the CALTECH II model¹⁶ using a shower coupled to a string decaying into clusters. The aplanarity distribution shows once more the lack of highly aplanar events in the fixed-order QCD model. On the other hand, the mere use of a parton shower is no guarantee for success: the CALTECH II model, and to a lesser extent the Webber model, overshoot the data for large aplanarities. Similarly, those two models fail in reproducing the thrust distribution over the full range. Compared to these event shape variables, inclusive spectra prove to be much more forgiving: for example, all models achieve a reasonable description of the distributions in momentum and in transverse momentum with respect to the jet axis. (Fig. 9; slight problems in the modeling of the large- x data above $x \approx 0.8$ should not be taken too seriously, since in this region MARK II and HRS³⁴ data differ somewhat). The model comparison is summarized in an overall chi-squared describing the agreement between data and model for 18 distributions with a total of 450 data points³⁵. The Lund shower model emerges as a clear winner with a χ^2 of 960, followed closely by the 2nd order version with a χ^2 of 1230. This indicates that while some specific distributions show clearly the need for parton showers at PEP energies, most features of the events are still well represented by 2nd order QCD plus string fragmentation. The Webber model comes in third, with a χ^2 of 2870. The discrepancies with the data are almost entirely due to the cluster algorithm; the shower formalism of the Webber model combined with a Lund string reproduces the success of the Lund model. The situation is different for the CALTECH model: neither replacement of the shower part nor replacement of the hadronization part can reduce its high χ^2 of 6830 to competitive values.

In summary, data seem to indicate a clear preference for string models with normal mesons and baryons (instead of heavy clusters) as primary hadrons. On the other hand, it is not yet obvious if the concept of a cluster itself is at fault, or if simply the present implementations of cluster production and decay are inappropriate. An interesting by-product of the investigation is the evidence for a very low cutoff in the perturbative evolution of a parton shower: the optimum cutoffs for parton virtualities are determined to be 1 GeV for the Lund model and 0.75 GeV for the Webber model!

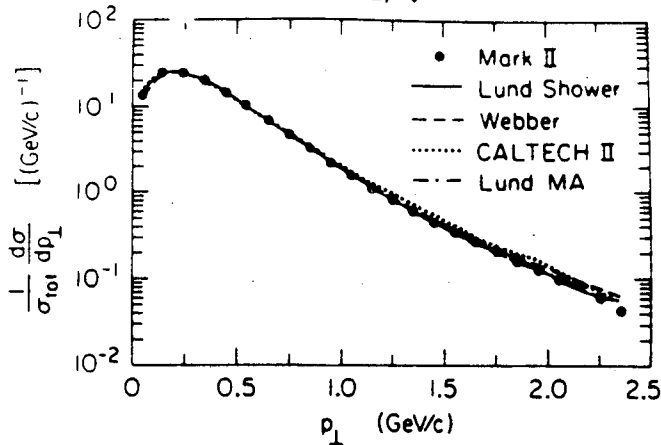
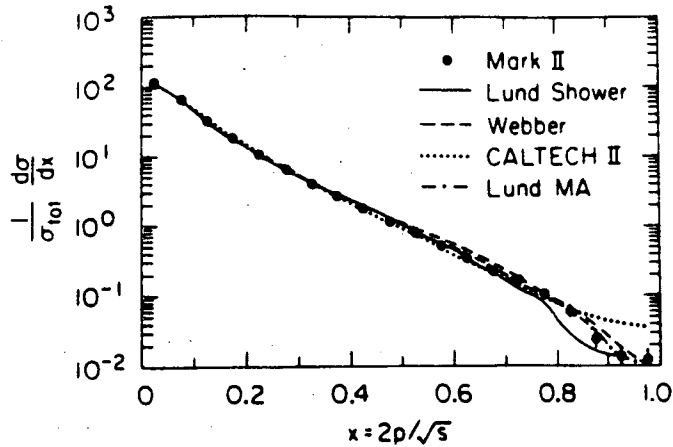
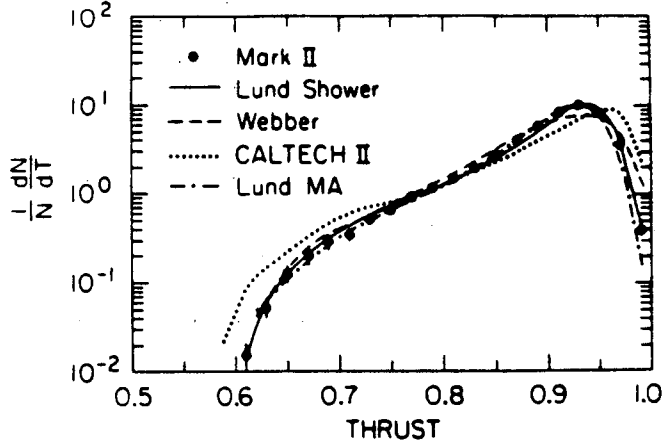
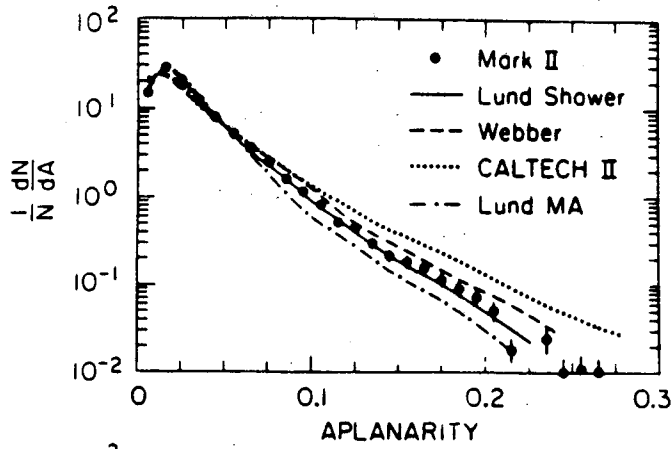


FIGURE 8

Normalized distribution in aplanarity and thrust of e^+e^- annihilation events at $\sqrt{s}=29$ GeV, compared to predictions of the Lund string model with parton showers (full line), the Webber model (dashed), the CALTECH II model (dotted) and the Lund model using 2nd order QCD matrix elements (dash-dotted). From MARK II³³.

FIGURE 9

Single particle distributions in $x=2p/\sqrt{s}$ and transverse momentum w/r to the thrust axis, compared to model predictions (see Fig. 8). From MARK II³³.

7. THE PARTICLE COMPOSITION OF JETS

Whereas the global structure of the events is dominated by properties of the parton distribution in the events (at least at PEP/PETRA energies or above), the particle composition of the final state is mainly sensitive to the modeling of the nonperturbative phase. Measurements of the particle composition of jets provide further constraints for models of this 2nd stage of parton fragmentation. In cluster models, the particle composition is related to the cluster mass spectrum, with the cluster decay being described by phase space or parametrized according to low-energy data. By contrast, most versions of string models put in particle composition more or less by hand via a large number of parameters, describing a) the frequencies with which different flavors of partons (light quarks, strange quarks or diquarks) are produced in the decay of the string, and b) the probabilities for two partons to recombine into different hadron (spin) states. Based on world-averages of data on pseudoscalar and vector meson and on octet and decuplet baryon multiplicities in e^+e^- annihilation around 30 GeV, one finds the parameter values listed in table 1³⁶ (within the Lund framework):

Table 1: Lund parameters determining particle composition

strange quark suppression	$s/u = 0.29 \pm 0.02$
diquark suppression	$qq/q = 0.09 \pm 0.01$
spin-1 diquark suppression	$\frac{1}{3}qq_1/qq_0 = 0.05 \pm 0.04$
extra strange diquark suppression	$(us/ud)/(s/d) = 0.7 \pm 0.3$
fraction of pseudoscalar mesons	
for u,d quarks	$p/(v+p) = 0.41 \pm 0.05$
for s quarks	$p/(v+p) = 0.45 \pm 0.05$
for c quarks	$p/(v+p) = 0.62 \pm 0.08$

Experience with different versions of string models proves that these parameters are very insensitive to the simulation of the early perturbative stages of the fragmentation process; fixed order string models and shower models use (almost) identical parameters for best agreement with the data, and predict very similar spectra (in the following, I will therefore often mention "Lund predictions" without specifying model versions etc.). The dynamics of hadron production in a color string explains qualitatively the deviations of the measured parameters from their "natural values" expected for SU(6) symmetry, such as $s/u = 1$ and $p/(v+p) = 1/4$. For example, due to the finite energy density in the string, the production of heavier quarks is suppressed³⁷. The preference of pseudoscalar meson states over vector meson states (taking the spin factor into account) is simply a consequence of the lower mass of the pseudoscalars¹².

New e^+e^- data allow one to push the model tests further: pion, kaon and proton cross sections from the TPC detector³⁸ finally cover most of the kinematic range with reasonable precision (Fig. 10). In the region of overlap, the agreement with previous TPC³⁹ and TASSO⁴⁰ data is good. Also included in Fig. 10 are new π^0 cross sections from TASSO⁴¹, which are in perfect agreement with the charged-pion cross sections. Lund model predictions fit the data quite well, except for the large- x proton cross sections. This is even more evident from the corresponding charged-hadron fractions shown in Fig. 11: even for large variations of the parameters it is hard to obtain perfect agreement between Lund model and data, as far as the x -dependence of the proton fraction is concerned (as of this date, however, not all possibly relevant parameters have been fully explored). On the other hand, models such as CALTECH II fail much more spectacularly. The rise of proton fractions with x in most models is caused by the treatment of baryons as being composed effectively of two constituents, a quark and a diquark, thereby treating mesons and baryons on the same footing. Kinematical effects then cause the heavier baryon to retain a larger share of the initial quarks energy. Somewhat as a surprise, proton fractions in the Webber model turn over near $x \approx 0.5$ and go to zero for $x \approx 1$, as predicted e.g. by dimensional counting rules⁴² due to the larger number of constituents in a baryon. It is not obvious why the two cluster models - Webber and CALTECH II - behave so differently.

Also new are detailed measurements of the inclusive η cross section. The η is interesting since in the Lund model the η production rate is closely tied to the rates of pions and kaons, the other members of the nonet; a serious failure of the model would indicate the need for even more *ad hoc* parameters, and lessen the confidence in the model's predictive power. Exactly such a failure appears to be evident from the HRS data⁴³; the measured η multiplicity of 0.37 ± 0.08 is a factor two below the predictions of about 0.7-0.8 η 's per event (see also Fig. 12). The HRS data and an older JADE result⁴⁴ of 0.64 ± 0.15 η 's per event are marginally consistent. At the same time, however, the ARGUS group finds 0.42 ± 0.16 η 's per event in their annihilation data in the continuum near $\sqrt{s} = 10$ GeV⁴⁵, well consistent with the Lund prediction of 0.45. The comparison indicates either a completely anomalous energy dependence of η production, or a problem in one (or both) of the experimental analyses. I'm strongly inclined to believe in the latter, and comparing the quality of the η signals from the two experiments (Fig. 13), it appears somewhat premature to dig into the Lund Monte Carlo code and install an extra η suppression factor⁴⁶.

Finally, there are now e^+e^- data accumulating on mesons with orbital angular momentum. Table 2 summarizes HRS results⁴⁷ at $\sqrt{s} = 29$ GeV, including their new $K^*(892)$ data for comparison. Also included are relevant results from the Upsilon region around 10 GeV⁴⁸.

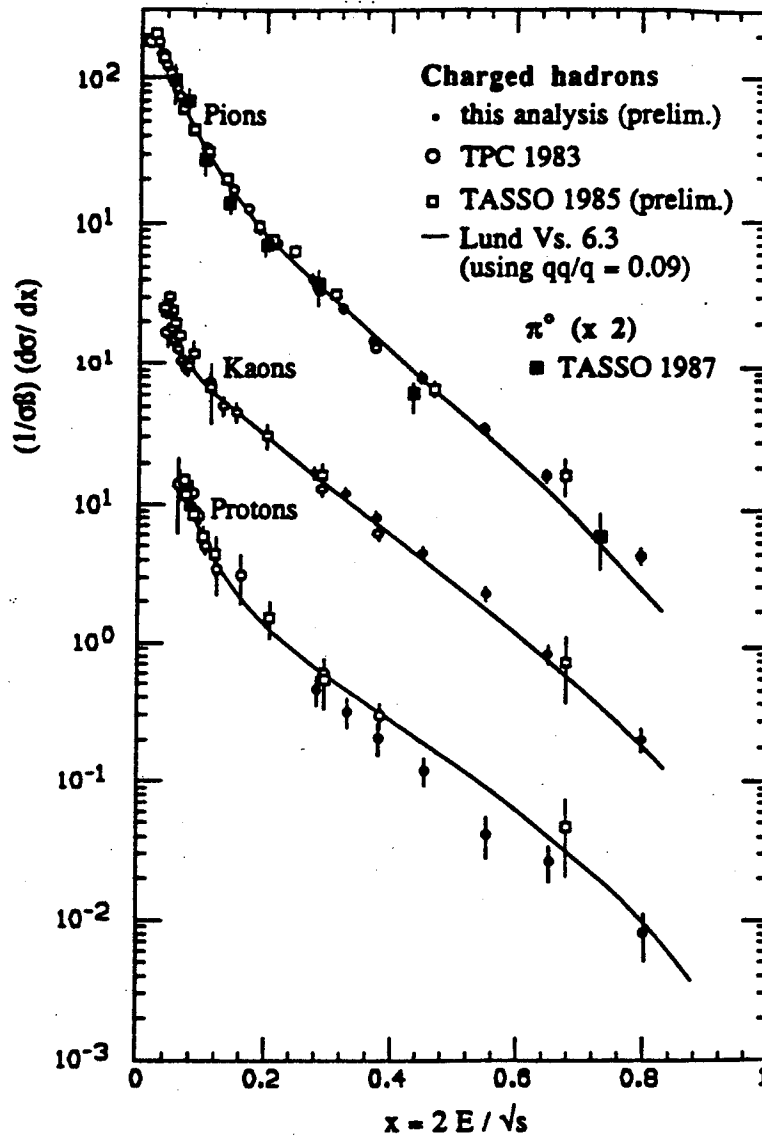


FIGURE 10

Cross section $(1/\sigma\beta)(d\sigma/dx)$ for inclusive production of pions, kaons and protons (+c.c.) in e^+e^- annihilation around $\sqrt{s}=30$ GeV, as a function of $x=2E/\sqrt{s}$. Shown are new³⁸ and old³⁹ TPC/ 2γ data as well as TASSO⁴⁰ data. Full lines give predictions of the Lund model (using $qq/q=0.09$). Also shown is a new measurement of π^0 cross sections by TASSO⁴¹.

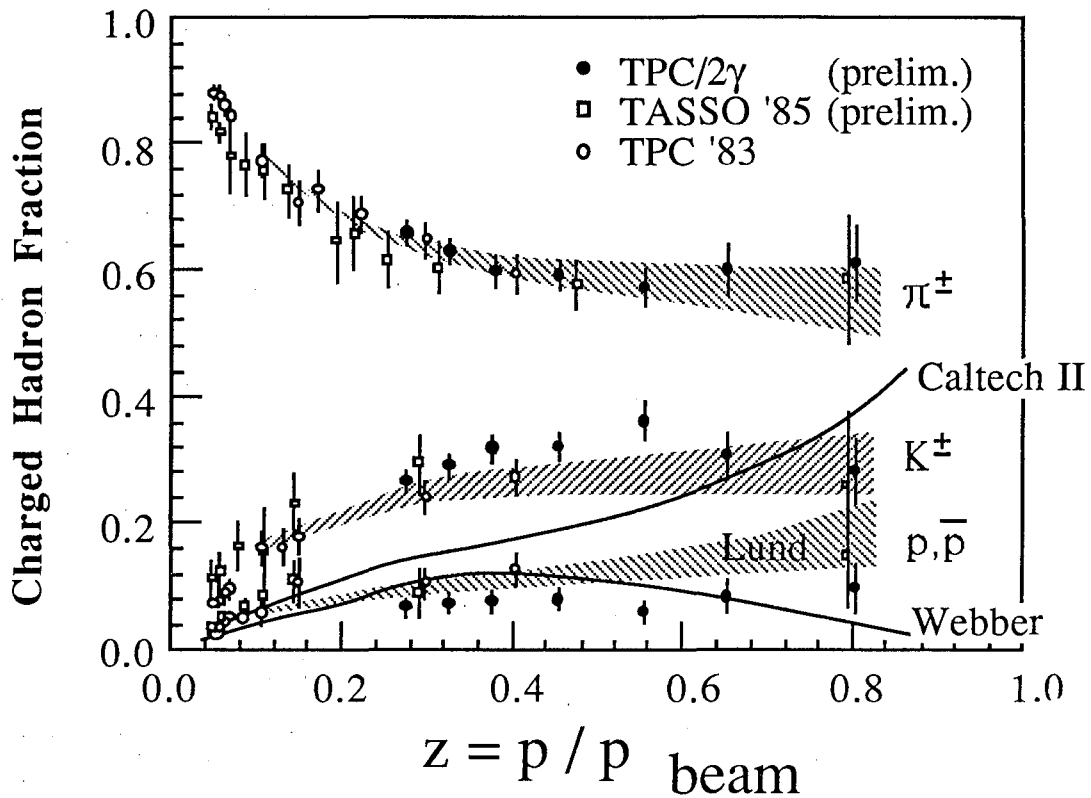


FIGURE 11

Fraction of charged pions, kaons and protons in e^+e^- annihilation around $\sqrt{s}=30$ GeV, as a function of z . Shown are new³⁸ and old³⁹ TPC/2 γ data as well as TASSO⁴⁰ data. Shaded areas indicate the range of Lund model predictions for different model parameters. Also included are predictions of the Webber and CALTECH II models for the proton fraction.

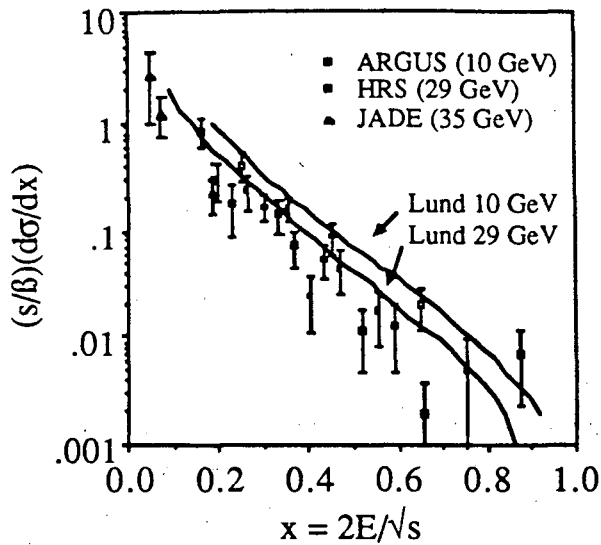


FIGURE 12
Cross section $(s/\beta)(d\sigma/dx)$ for inclusive production of eta mesons in e^+e^- annihilation at $\sqrt{s}=29$ GeV (HRS⁴³), at 34 GeV (JADE⁴⁴) and around 10 GeV (ARGUS⁴⁵). Full lines indicate Lund model predictions for 10 and 29 GeV.

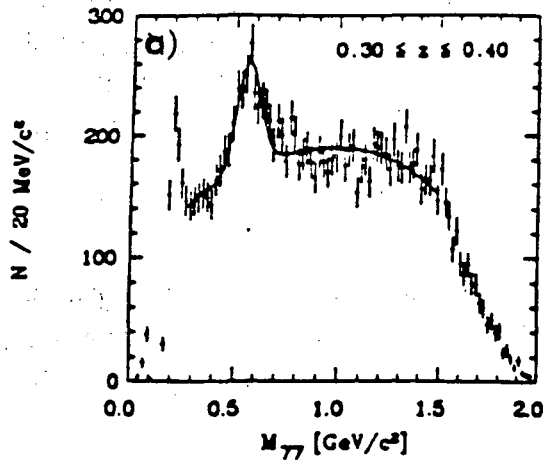


FIGURE 13
Two-photon invariant mass distributions (a) from the ARGUS experiment⁴⁵ for $0.3 < x_{\gamma\gamma} < 0.4$ and (b) from the HRS experiment⁴³ for $p_{\gamma\gamma} > 5$ GeV.

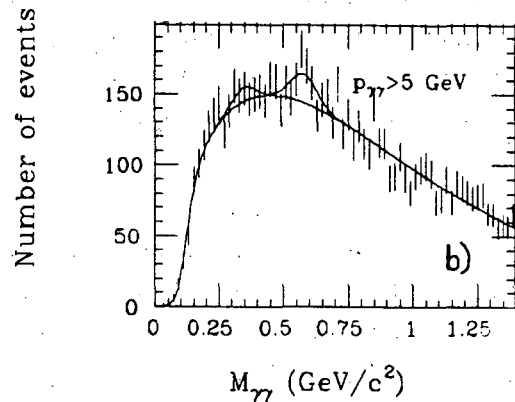


FIGURE 14
Inclusive cross section $(s/\beta)(d\sigma/dx)$ for $f_2(1270)$ and $K^*(1430)$ production in e^+e^- annihilation at $\sqrt{s}=29$ GeV, as a function of $x=2E/\sqrt{s}$. Lines indicate predictions of the Webber model. From HRS⁴⁷.

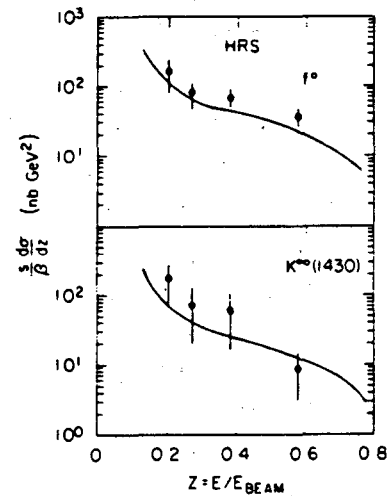


Table 2: Inclusive rates for $l=1$ mesons

Meson	JPC	Rate/event	Ref.
$f_2(1270)$	2^{++}	0.14 ± 0.04	HRS
$K^{*\pm}(1430)$	2^+	0.09 ± 0.03	HRS
$K^{*0}(1430)$	2^+	0.12 ± 0.06	HRS
$f_0(975)$	0^{++}	0.06 ± 0.03	HRS
$D^{*0}(2420)/D^{*+}$		0.17 ± 0.09	ARGUS
$D^{*0}(2420)/D^{*+}$		0.12 ± 0.05	CLEO

Typical rates for $L=1$ mesons are around 0.1 per event, corresponding to 10-20% of the production rate for vector mesons. A similar ratio is obtained for charmed mesons. This seems to imply that $L=1$ mesons are not a dominant source of stable hadrons; only 7% of all kaons originate from $K^*(1430)$, compared to 42% from $K^*(892)$. The fact that $L=1$ meson production is neglected e.g. in the Lund model should hence not cause major problems. The $K^*(1430)$ to $K^*(892)$ ratio can be understood qualitatively both in the string framework (with about 1 fm between string breaks and typical transverse momenta around 300 MeV it is easy to create one unit of orbital angular momentum, but the $L=1$ wave function disfavors quark recombination into such states), and within the cluster framework, where heavy mesons are suppressed by phase space (Fig. 14).

8. BARYON PRODUCTION IN JETS

While detailed data on inclusive meson cross sections and particle composition certainly provides valuable constraints and guidelines for the construction of fragmentation models, it is often hard to find the relation to the underlying physics, mainly since virtually nothing can be derived from first principles and since there are usually many parameters and effects which influence any given distribution. A more powerful tool may be the study of baryon production, which offers several interesting features:

- As evidenced in Fig. 11, models differ widely in their predictions for baryon rates, much more than in the meson sector.
- Baryons provide a more direct probe of the confinement process. Most pions are created in resonance decays, rather than as primary hadrons during the color confinement. As a result, the reconstruction of the primary production process using final pions is a difficult task. For example, the rms rapidity difference between a pion and its first-generation ancestor is about 0.5 units, comparable to the length of typical rapidity correlations. Protons, on the other hand, are directly produced in more than 50% of the cases, and have an rms rapidity difference to their ancestor of only 0.08 units, thus preserving all primary correlations. (The numbers given here refer to the Lund model; however, the qualitative arguments hold independently of details of the modeling.)

- Finally, the possibility to vary the number of strange quarks in a baryon between 0 and 3 provides an improved lever arm for studies of the flavor dependence of cross sections.

The second point given above also applies to heavier mesons; however, those cannot be identified with sufficient purity to go beyond inclusive studies.

Before using baryon spectra and correlations between baryons to study confinement, one needs to demonstrate that baryons are indeed a direct product of the hadronization process, and not just decay products of heavy meson-like states, as proposed e.g. in early versions of the Webber model. Relevant data was published by the TPC group⁴⁹, and is now available with significantly improved statistics. The analysis uses events with at least one proton and one antiproton; Fig. 15 shows the distribution in $|\cos\theta|$ for these pairs, after subtraction of random combinations. Here θ is the angle between proton momentum and jet axis, measured in the $p\text{-}\bar{p}$ rest frame. Baryons from meson decay should yield a flat distribution in $|\cos\theta|$, quite in contrast with the experimental data, which is peaked near $|\cos\theta|\approx 1$ and proves that baryons are sensitive to the direction of the initial color field and are therefore produced during and not after the confinement process.

The same data set has been used to study rapidity correlations between baryons⁵⁰. Among the results is further evidence for the local conservation of baryon number: the net excess of baryon number per unit rapidity in events with a "trigger" antibaryon at a given fixed rapidity peaks at the rapidity of the trigger particle. Examples for a trigger- \bar{p} around $y\approx 0.6$ and for a trigger- $\bar{\Lambda}$ near $y\approx 1.3$ are shown in Fig. 16(a) and (b). Local conservation of baryon number is expected in most fragmentation models; a more interesting feature shows up in rapidity correlations between two antiprotons⁵¹ or between an antiproton and an antilambda (Fig. 17). The correlation function C is defined as usual:

$$C = \left(\frac{1}{\sigma} \frac{d^2\sigma}{dy_a dy_b} \right) / \left(\frac{1}{\sigma^2} \frac{d\sigma}{dy_a} \frac{d\sigma}{dy_b} \right) - 1$$

This definition yields $C=0$ for uncorrelated production obeying Poisson statistics. Like in Fig. 16(a), one \bar{p} is fixed near $y_a\approx 0.6$ and C is displayed as a function of the rapidity y_b of the other antibaryon. We observe a large negative correlation between antibaryons of similar rapidity or, in other words, a "repulsion" between two antibaryons. The range of the effect for $\bar{p}\bar{p}$ is far too big to be attributed to Fermi-Dirac statistics, assuming usual source sizes of about 1 fm. The phenomenon is reproduced by the late versions of the Lund model ("symmetric Lund"), whereas earlier versions ("standard Lund") or the Feynman-Field (FF) model (upgraded to include baryon production⁵²) fail to describe the data. The lesson to be learned is simple: particle production is usually pictured via a chain of new quark-antiquark pairs spanned between the initial quarks (Fig. 18(a)). The standard (and so far only successful) implementa-

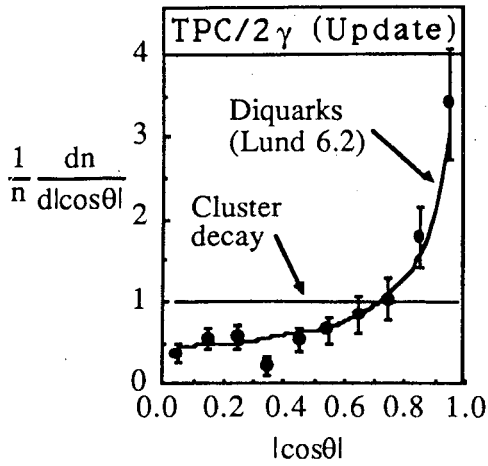


FIGURE 15

Distribution in $|\cos\theta|$ of proton-antiproton pairs produced in e^+e^- annihilation at $\sqrt{s}=29$ GeV, after background subtraction. θ is the angle between the proton momentum and the jet axis, measured in the proton-antiproton rest frame. Lines give model predictions for proton production via a diquark mechanism and via cluster decay. From TPC/2 γ .

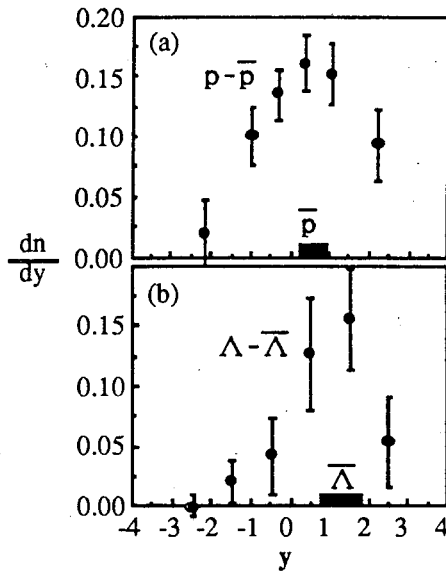


FIGURE 16

(a) Net baryon number density observed in e^+e^- annihilation events with an antiproton near $y=0.6$. The baryon number density is defined as the number of protons per event and unit rapidity minus the number of antiprotons. (b) As (a), but using lambdas, and for a higher rapidity $y=1.3$ of the "trigger"-antilambda. From TPC/2 γ ⁵⁰.

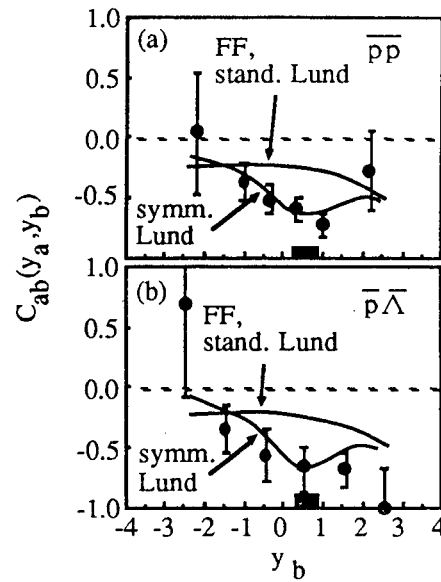


FIGURE 17

(a) Correlation function between an antiproton at $y_a \approx 0.6$ and another antiproton at y_b , as a function of y_b . Lines show predictions of the Lund model using the symmetric fragmentation function and using Feynman-Field or standard Lund fragmentation functions. (b) as (a), but showing the correlation between an antiproton at $y_a \approx 0.6$ and an antilambda at y_b . From TPC/2 γ ⁵⁰.

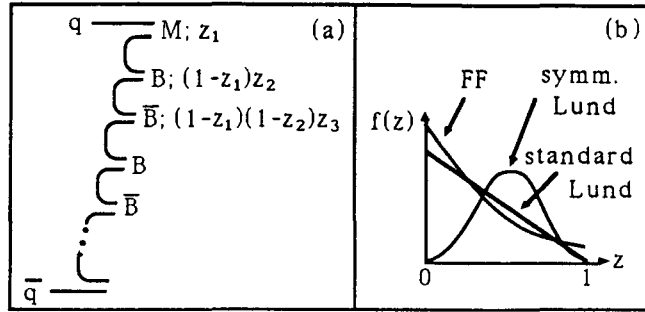


FIGURE 18

(a) Hadronization chain resulting in the production of two baryons and two antibaryons. (b) Fragmentation function $f(z)$ describing the energy sharing between hadron H and remaining parton (quark or diquark) p' in the basic process $p \rightarrow H(z) + p'(1-z)$ in iterative fragmentation models, for the symmetric Lund, standard Lund, and Feynman-Field models.

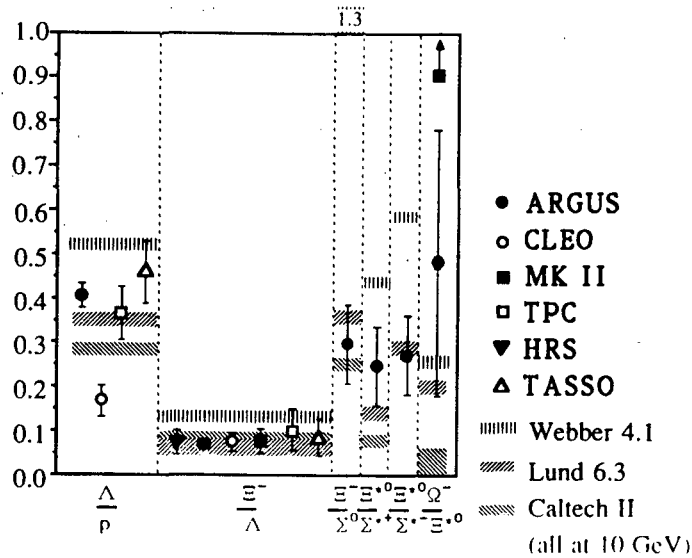


FIGURE 19

Strangeness suppression in baryon production. Shown are ratios of baryon production cross sections for strangeness $s+1$ and s ($s=0,1,2$), for baryons belonging to the same spin multiplet. Feed down due to decays is not corrected and affects mainly p and Λ rates. Data on e^+e^- annihilation in the continuum near $\sqrt{s}=10$ GeV from ARGUS and CLEO, and around $\sqrt{s}=30$ GeV from MARK II, TPC/ 2γ , HRS and TASSO⁶⁰⁻⁶². Shaded bands represent predictions of the Lund, Webber and CALTEC II models (for $\sqrt{s}=10$ GeV).

tion of baryon production is via occasional production of diquark-antidiquark pairs⁵³; natural mechanisms to achieve this have been described e.g. in ref.⁵⁴. Obviously, quantum numbers such as charge, strangeness or baryon number will alternate along the chain; it is impossible for two neighboring particles to have the same (non-zero) charge, strangeness or baryon number. Provided that rapidity y and rank in the chain are closely correlated, this would explain the anticorrelation between two antibaryons. The mapping between rank and rapidity is governed by the function $f(z)$ which (in an iterative implementation) determines which fraction of the available energy goes into the next hadron^{12,55}. Both the "standard" Lund model and the FF model use $f(z)$'s which peak at $z=0$ (Fig. 18(b)). This means that it is likely that a hadron receives a small energy fraction, leaving a lot for the remainder of the chain and making it not too unlikely that a later hadron will obtain more energy and end up at a higher rapidity. In other words, the correspondence between rank in the chain and rapidity is rather poor. This changes for the "symmetric" Lund model, with $f(z) = \frac{(1-z)^a}{z} e^{-bm^2/z}$. In particular for heavy hadrons, this function exhibits a pronounced peak at intermediate z and goes to zero for small z . Such an $f(z)$ tends to give each (heavy) hadron an almost fixed fraction of the available energy, resulting in a tight correlation between rank and rapidity, and in an anticorrelation between particles with identical (charge-like) quantum numbers. The effect is invisible for pions, since for small masses the "symmetric" $f(z)$ also peaks near $z=0$ and is similar in shape to the function used in the "standard" Lund model, and since resonance decays and Bose-Einstein enhancements cover the anticorrelation even further. In conclusion, the observed effect provides strong support for the "symmetric" fragmentation function derived by the Lund group⁵⁶ and others⁵⁷.

9. FLAVOR DEPENDENCE OF BARYON RATES

I will now turn to the dependence of inclusive baryon production rates on the quantum numbers of the baryon. New data from PEP and PETRA include Ξ^- and Ω^- rates and a limit on Ξ^{*0} production in e^+e^- annihilation at 29 GeV from the MARK II⁵⁸ and data on $\Sigma^{*\pm}$ and Ξ^- from the HRS group⁵⁹:

Table 3: New data on baryon rates at $\sqrt{s} = 29$ GeV

MARK II	Ξ^-	0.017 ± 0.006
"	Ξ^{*0}	< 0.006 (90% CL)
"	Ω^-	0.014 ± 0.007
HRS	Ξ^-	0.016 ± 0.006
"	$\Sigma^{*\pm}$	0.033 ± 0.010

The Ξ^- rates agree well with each other and with earlier measurements⁶⁰. It is however surprising that the Ω^- rate is found to be larger than the Ξ^{*0} rate, and comparable to the Ξ^- rate. Given that decuplet baryons are believed to be strongly suppressed and that the Ω^- contains one more strange quark than the Ξ^- , one would expect at least an order of magnitude difference between the Ω^- and Ξ^- rates. Indeed, the ARGUS collaboration⁶¹ obtains at $\sqrt{s} = 10$ GeV the ratio $\Omega^-/\Xi^- = 0.11 \pm 0.06$, compared to the MARK II value of 0.8 ± 0.5 . The problem is clearly related to the Ω^- rate and not to the Ξ or Ξ^* rates, as demonstrated in a comparison with Λ rates (which are well-measured and unambiguously established): $\Omega^-/\Lambda = 0.07 \pm 0.03$ (MARK II) vs $\Omega^-/\Lambda = 0.008 \pm 0.004$ (ARGUS). If the Ω^- rate obtained at 29 GeV were taken literally, it would point to an unexpectedly large energy dependence in the baryon composition; on the other hand, the MARK II and ARGUS numbers are of course compatible within 2 S.D. .

Instead of further discussing individual cross sections, let us investigate the dependence of cross sections on the number of strange quarks in a baryon by forming cross section ratios for members of the same multiplet, such that the particle in the numerator has one additional strange quark compared to the particle in the denominator (Fig. 19, including previous results and lower-energy data from CLEO and ARGUS^{60,61,62}). Except for the Ω^-/Ξ^{*0} ratio and a Λ/p point from CLEO, there is good agreement between different experiments and cms energies. The additional strange quark causes a reduction of the rates by about 0.3, as seen for the heavier baryons which are dominantly directly produced (as compared to Λ and p , where rates are dominated by feeddown from decays). Also included in Fig. 19 are bands corresponding to predictions of the Lund, Webber and CALTECH II Monte Carlos at 10 GeV cms energy. The Lund model describes the data reasonably well, whereas the Webber model is systematically somewhat high, indicating that the suppression of strange baryons due to cluster decay phase space alone might not be sufficient. The CALTECH II model underpredicts most ratios. The distinction between models is more obvious from at the spin-dependence of cross sections: Fig. 20 shows ratios of decuplet and octet production rates of baryons with the same number of strange quarks. A strong suppression of decuplet particles is obvious, even allowing for the feeddown, which is not corrected for. Comparison with Webber model predictions demonstrates once more the existence of dynamical suppression mechanisms beyond cluster decay phase space.

10. STRING MODELS: NEW IDEAS

The color string model of parton fragmentation is highly successful and has proven a fertile ground for extensions, which may ultimately eliminate some of the

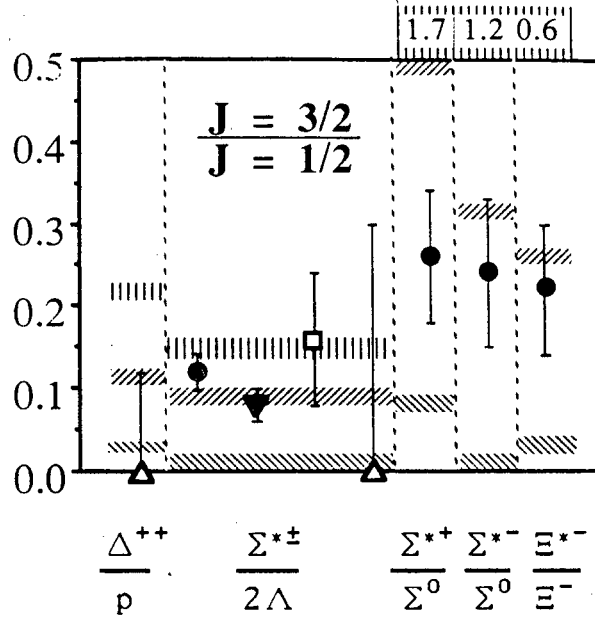


FIGURE 20

Ratios of inclusive production rates for decuplet and octet baryons. Only baryons with the same strangeness content are compared. See Fig. 19 for explanation of symbols.

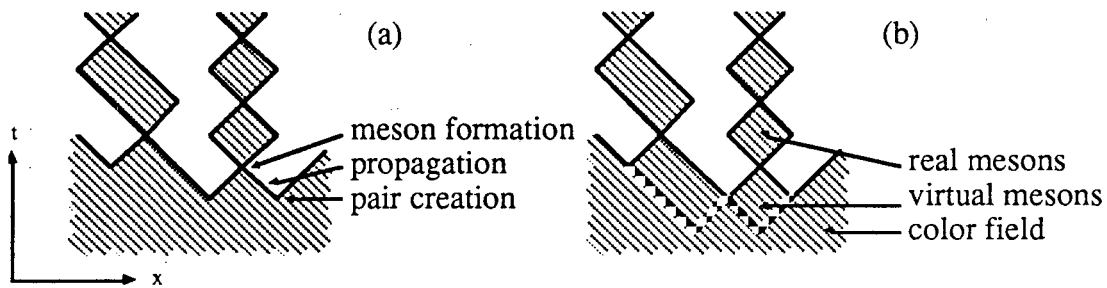


FIGURE 21

Space-time diagrams describing hadron production in string models: (a) conventional formulation based on the string \rightarrow quarks, quarks \rightarrow mesons transition in a one-dimensional system of massless quarks and (b) alternative description as a direct transition string \rightarrow mesons.

problems with the model such as the ever increasing number of parameters. I will discuss one such extension in detail.

As mentioned before, the production of hadrons is basically described as a two-step process: quark production followed by recombination into hadrons. Parton production and particle composition are governed by *ad hoc* parameters, whereas the momentum distributions are given by the mass-dependent symmetric fragmentation function $f(z,m) = \frac{(1-z)^a}{z} e^{-bm_T^2/z}$ discussed in connection with the baryon correlations. Given that quark production and recombination involve similar time scales, and that in a quantum mechanical description of the process the production probability of a given quark will depend on the wave function of the final bound state, one may try the alternative approach of a string coupling directly to hadrons. The basic idea is illustrated in Fig. 21, which shows the usual space-time diagram describing quark pair production in the string, propagation of quarks until they meet a partner, and then propagation in a "yoyo" mode as a bound meson (Fig. 21(a)). Equally well, one can however view the stage of propagation of the quark as part of the first oscillation of the meson "yoyo" (Fig. 21(b)); from this point of view it appears that the color flux tube as a whole undergoes a transition into meson states, without an intermediate quark stage. Of course, due to the uncertainty relation the two views cannot really be distinguished, but the question remains as to which (if any) is the more appropriate classical analogue.

In the framework of Fig. 21(b), only the hadron mass is left as a quantity to govern cross sections. One might speculate that the fragmentation function given above describes not only the x distribution for a given hadron flavor and given p_T , but that it also governs, via the (transverse) mass dependence, the particle composition³⁶ and the transverse spectra^{36,63}. In this case, the two parameters a and b (instead of the usual dozen parameters) account for the suppression of large transverse momenta, of vector mesons, of strange mesons and of baryons. Such a modification of the Lund string model has been studied in Ref. 36. More or less by construction, this ("UCLA"-) model retains inclusive distributions predicted by the Lund model. Amazingly enough, it predicts hadron rates for non-strange and strange mesons and baryons correctly within about 30-40%, over a range of more than 3 orders in magnitude between common (π) and very rare (Ω) particles (Fig. 22). Transverse-momentum spectra are also reproduced well. While there are certainly open questions concerning details of the implementation of this model, it demonstrates that present data cannot be used to prove conclusively that the suppression of strange hadrons and baryons actually occurs at the quark level. Much more precise measurements of production rates are needed for a better distinction!

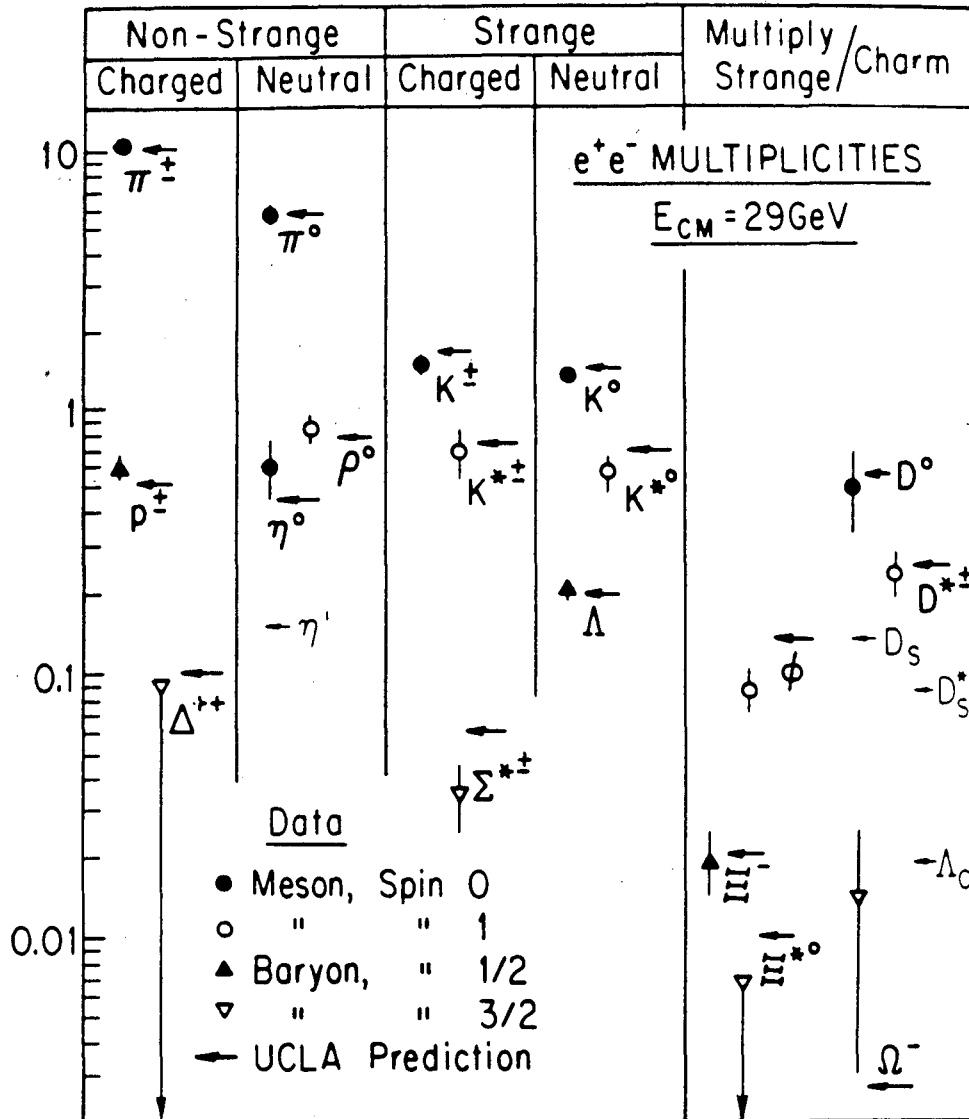


FIGURE 22

Predictions of the UCLA model³⁶ for hadron production rates in e^+e^- annihilation at $\sqrt{s}=29$ GeV (arrows), compared to experimental data (averaged over detectors, where available). The two model parameters a and b are tuned for optimum agreement with the data, resulting in $a=1.1$ and $b=0.75$ GeV⁻² (in the Lund Vs. 6.2 framework).

11. SUMMARY

While the study of the physics of jets during the last years has not given rise to revolutions in our understanding of the strong interaction, it is certainly characterized by a steady and evolutionary progress.

Even at PEP and PETRA energies, we are now finding evidence for QCD effects beyond the 2nd order calculations, and see the effects of parton showers evolving down to very low cutoffs and large numbers of emitted gluons. Coherence phenomena offer a bridge between shower and string phenomenology.

String fragmentation models with normal mesons and baryons as primary particles (as opposed to clusters) are definitely preferred by the data, and at the same time provide a powerful framework for extensions such as the "UCLA-model" for particle composition.

Baryons are emerging as a powerful tool to study the hadronization process, and are likely to provide deeper insight into the fragmentation process as soon as sufficiently large data samples are available; first results look very promising.

ACKNOWLEDGEMENT

This work was supported by the U.S. Department of Energy under Contract No. DE-AC03-76SF00098. The author acknowledges receipt of an A.P. Sloan Fellowship.

REFERENCES

- 1 K. Konishi, A. Ukawa and G. Veneziano, Phys. Lett. 78B (1978) 243; 80B (1979) 259; P. Cvitanovic, P. Hoyer, K. Zalewski, Nucl. Phys. B176 (1980) 429
- 2 G. Altarelli and G. Parisi, Nucl. Phys. B126 (1977) 298
- 3 A.H. Muller, Phys. Lett. 104B (1981) 161; B.I.Ermolaev and V.S. Fadin, JETP Lett. 33 (1981) 269; A. Basetto, C. Ciafaloni and G. Marchesini, Phys. Rep. 100 (1983) 201; G. Marchesini and B.R. Webber: Nucl. Phys. B238 (1984) 1
- 4 D. Amati and G. Veneziano, Phys. Lett. 83B (1979) 87
- 5 Using the Lund Monte Carlo Jetset 6.3 with default parameters
- 6 The name "cluster model" for QCD shower models is somewhat of a historical misnomer, since recent versions of string models also produce clusters as primary objects, while on the other hand recent shower models create both ordinary particles and clusters in the preconfinement process.
- 7 B.R. Webber, Nucl. Phys. B238 (1984) 492
- 8 G.C. Fox and S. Wolfram: Nucl. Phys. B168 (1980) 285
- 9 R.D. Field and S. Wolfram: Nucl. Phys. B213 (1983) 65
- 10 T.D. Gottschalk, Nucl. Phys. B239 (1984) 349
- 11 The actual number of "free" parameters in a model is sometimes hard to determine, since some of the parameters e.g. in the Lund model have virtually no influence on the simulation; they are included as parameters for the sole reason to demonstrate that the model is insensitive to these quantities.
- 12 B. Andersson et al., Phys. Rep. 97 (1983) 31
- 13 X. Artru, Phys. Rep. 97 (1987) 1; A. Casher, H. Neuberger and S. Nussinov, Phys. Rev. D20 (1979) 179; D21 (1980) 1966
- 14 J. Schwinger, Phys. Rev. 128 (1962) 2425
- 15 T. Sjöstrand, Computer Phys. Comm. 39 (1986) 347; 28 (1983) 229; 27 (1982) 243
- 16 T.D. Gottschalk and D.A. Morris, Nucl. Phys. B288 (1987) 729
- 17 T.D. Gottschalk, Nucl. Phys. B239 (1984) 325
- 18 M. Bengtsson and T. Sjöstrand, Nucl. Phys. B289 (1987) 810; G. Marchesini, Proc. UCLA Workshop on Standard Model Physics at the SSC, ed. H.U. Bengtsson et al., p 114 (1986)
- 19 P. Hoyer et al., Nucl. Phys. B161 (1979) 349
- 20 A. Ali et al., Phys. Lett. 93B (1980) 155

- 21 S. Bethke, XXIII Int. Conf. on High Energy Physics, Berkeley, CA, 1986, Ed. S.C. Loken, p. 1079
- 22 T. Gottshalk and M.P. Shatz, Phys. Lett. 150B (1985) 451
- 23 F. Gutbrod et al., Z. Phys. C35, 534 (1987)
- 24 H.J. Behrend et al. (CELLO), Phys. Lett. 138B (1984) 311
- 25 Sau Lan Wu, Talk at the Int. Symp. on Lepton and Photon Interactions at High Energies, Hamburg, 1987
- 26 H.J. Behrend et al. (CELLO), Phys. Lett. 183B (1987) 400 and paper submitted to the Int. Symp. on Lepton and Photon Interactions at High Energies, Hamburg, 1987
- 27 W. Bartel et al. (JADE), paper submitted to the Int. Symp. on Lepton and Photon Interactions at High Energies, Hamburg, 1987
- 28 W. Bartel et al. (JADE), Z. Phys. C33 (1986) 23
- 29 W. Braunschweig et al. (TASSO), paper submitted to the Int. Symp. on Lepton and Photon Interactions at High Energies, Hamburg, 1987
- 30 Ya. I. Azimov et al., Phys. Lett. 165B (1985) 147
- 31 W. Bartel et al. (JADE), Phys. Lett. 101B (1981) 129; 134B (1984) 275; 157B (1985) 340; H. Aihara et al. (TPC), Z. Phys. C28 (1985) 31; M. Althoff et al. (TASSO), Z. Phys. C29 (1985) 29
- 32 H. Aihara et al. (TPC), Phys. Rev. Lett. 57 (1986) 945; P. Sheldon et al. (MARK II), Phys. Rev. Lett. 57 (1986) 1398; W. Bartel et al. (JADE), paper submitted to the Int. Symp. on Lepton and Photon Interactions at High Energies, Hamburg, 1987
- 33 A. Petersen et al. (MARK II), SLAC-PUB-4290 (1987)
- 34 D. Bender et al. (HRS), Phys. Rev. D31 (1985) 1
- 35 Note that correlations between data points in related distributions (such as thrust and sphericity) are taken into account in the calculation of χ^2 ; one should therefore not attempt to interpret the resulting χ^2 in a strictly statistical sense.
- 36 C.D. Buchanan and S.B. Chun, UCLA-87-005 (1987), subm. to Phys. Rev. Lett.
- 37 For reviews and further refs. see A. Wroblewski, Acta Phys. Pol. B16 (1985) 379; P.K. Malhotra and R. Orawa, Z. Phys. C17 (1983) 85; W. Hofmann, LBL-23921 (1987)

- 38 H. Aihara et al. (TPC), paper submitted to the Int. Symp. on Lepton and Photon Interactions at High Energies, Hamburg, 1987
- 39 H. Aihara et al. (TPC), Phys. Rev. Lett. 52 (1984) 577
- 40 M. Althoff et al. (TASSO), Z. Phys. C17 (1983) 5; and paper subm. to 1985 Int. Symp. on Lepton and Photon Int., Kyoto (1985)
- 41 W. Braunschweig et al. (TASSO), Z. Phys. C33 (1986) 13
- 42 S. Brodsky and G. Farrar, Phys. Rev. Lett. 31 (1973) 1153; V.A. Matveev et al, Nuovo Cimento Lett. 1 (1973) 719; S. Brodsky and J. Gunion, Phys. Rev. D17 (1978) 848
- 43 S. Abachi et al. (HRS), ANL-HEP-CP-87-60 (1987), submitted to the Int. Symp. on Lepton and Photon Interactions at High Energies, Hamburg, 1987
- 44 W. Bartel et al. (JADE), Z. Phys. C28 (1985) 343
- 45 A. Drescher, Ph. D. Thesis, Dortmund (1987)
- 46 Also, the MARK II experiment finds η rates consistent with the JADE data and with the Lund model. J. Dorfan, priv. comm.
- 47 M. Derrick et al. (HRS), Phys. Lett. 158B (1985) 519; S. Abachi et al. (HRS), Phys. Rev. Lett. 57 (1986) 1990; ANL-HEP-CP-87-71 (1987), submitted to the Int. Symp. on Lepton and Photon Interactions at High Energies, Hamburg, 1987
- 48 D.B. MacFarlane, Proc. XXIII Int. Conf. on High Energy Physics, Berkeley (1986), p. 664; C. Bebek et al. (CLEO), paper submitted to the Int. Symp. on Lepton and Photon Interactions at High Energies, Hamburg, 1987
- 49 H. Aihara et al. (TPC), Phys. Rev. Lett. 55 (1985) 1047
- 50 H. Aihara et al. (TPC), Phys. Rev. Lett. 57 (1986) 3140
- 51 In order to eliminate backgrounds from secondary protons, the study uses only antiprotons.
- 52 Using the Feynman-Field option provided in the Lund Monte Carlo.
- 53 B. Andersson, G. Gustafson and T. Sjöstrand, Nucl. Phys. B197 (1982) 45; T. Meyer, Z. Phys. C12 (1982) 77; E.M. Iglensfritz, J. Kripfganz and A. Schiller, Acta Phys. Pol. B9 (1978) 881; A. Bartl, H. Fraas and W. Majoretto, Phys. Rev. D26 (1982) 1061; for more refs. see B.O. Shytt, TRITA-FFY-87-04 (1987)
- 54 A. Casher, H. Neuberger and S. Nussinov, Phys. Rev. D20 (1979) 179; B. Andersson, G. Gustafson and T. Sjöstrand, Physica Scripta 32 (1985) 574
- 55 R.D. Field, R.P. Feynman, Nucl. Phys. B136 (1978) 1
- 56 B. Andersson, G. Gustafson and B. Söderberg, Z. Phys. C20 (1983) 317

- 57 M.G. Bowler, Z. Phys. C22 (1984) 155; C11 (1981) 169
- 58 S. Klein et al. (MARK II), Phys. Rev. Lett. 58 (1987) 664; SLAC-PUB-4338 (1987), subm. to Phys. Rev. Lett.
- 59 S. Abachi et al. (HRS), ANL-HEP-PR-87-26 (1987), subm. to the Int. Symp. on Lepton and Photon Interactions at High Energies, Hamburg, 1987
- 60 A. Galtieri, Proc. Int. Symp. on Multiparticle Dynamics, Lund, Sweden, 1984, p. 678; M. Althoff et al. (TASSO), Phys. Lett. 130 (1983) 340; Z. Phys. C26 (1984) 181
- 61 A. Albrecht et al. (ARGUS), paper subm. to the Int. Symp. on Lepton and Photon Interactions at High Energies, Hamburg, 1987
- 62 S. Behrends et al. (CLEO), Phys. Rev. D31 (1985) 2161
- 63 X. Artru, Z. Phys. C26 (1984) 83

*LAWRENCE BERKELEY LABORATORY
TECHNICAL INFORMATION DEPARTMENT
UNIVERSITY OF CALIFORNIA
BERKELEY, CALIFORNIA 94720*